Article ID: 1007-4627(2014) 02-0126-09

On the Slow Particles Production in Heavy Ion Induced Emulsion Interactions at Intermediate and High Energy

ZHANG Donghai, CHEN Yanling, WANG Guorong, LI Wangdong, WANG Qin, YAO Jijie, ZHOU Jianguo, LI Rong, LI Junsheng, LI Huiling

(*Institute of Modern Physics, Shanxi Normal University, Linfen 041004, Shanxi, China*)

Abstract: The multiplicity distributions and correlations of target fragments produced in 150 AMeV ^{4}He, 290 AMeV ^{12}C, 400 AMeV ^{12}C, 400 AMeV ^{20}Ne, and 500 AMeV ^{56}Fe induced different emulsion target interactions are investigated. It is found that the averaged multiplicity of grey track particle, black track particle and heavily ionized track particle increase with the increase of target size. There is a linear correlation between the multiplicity of different target fragments. The experimental results can be well explained based on the geometrical picture and the cascade evaporation model of nucleus-nucleus interactions.

Key words: heavy ion collision; target fragment; multiplicity; correlation; nuclear emulsion

CLC number: O571.6 **Document code:** A **DOI:** 10.11804/NuclPhysRev.31.02.126

1 Introduction

The multiplicity distributions and correlations of secondary particles are the basic experimental tools to study the mechanism of nucleus-nucleus interactions. Copious data have been obtained on hadron-nucleus[1−3] and nucleus-nucleus[4−27] interactions at relativistic and ultra-relativistic energies. A little investigation is made for interactions at intermediate and high energies (a few hundred MeV per nucleon)[28−31].

The geometrical aspects of nucleus-nucleus collisions can be understood in terms of the participant-spectator model[32−33]. According to this model, at finite impact parameters, three regions are produced after a collision between two nuclei. The participant region, the projectile spectator and the target spectator. The projectile spectator decays mainly into nuclear clusters since very little momentum transfer is required to form these fragments. Target spectator forms target fragments which include target recoiled protons (grey track particles) and target evaporated fragments (black track particles). The grey track particles are formed due to fast target protons of energy ranging up to 400 MeV. The black track particles are images of target evaporated particles of low-energy ($E < 30$ MeV) singly or multiply charged fragments.

In our recent investigation[31] the forward-backward multiplicity and correlations of target evaporated fragment and target recoiled proton produced in 150 AMeV ^{4}He, 290 AMeV ^{12}C, 400 AMeV ^{12}C, 400 AMeV ^{20}Ne and 500 AMeV ^{56}Fe induced different type of emulsion target interactions are studied, the general characteristics of the particle production in backward hemisphere and forward-backward multiplicity correlations in nucleus-nucleus collisions at intermediate and high energies are investigated. In this paper the multiplicity distributions and correlations of black, grey, and heavily ionized track particles produced in 150

Received date: 20 Apr. 2014; **Revised date:** 28 Apr. 2014

Foundation item: National Natural Science Foundation of China(11075100); Natural Science Foundation of Shanxi Province (2011011001-2); Shanxi Provincial Foundation for Returned Overseas Chinese Scholars(2011-58)

Biography: Zhang Donghai(1964–), male, Shanxi Wuzhai, Professor, working on the field of particle physics and nuclear physics; E-mail: zhangdh@dns.sxnu.edu.cn.

AMeV ^{4}He, 290 AMeV ^{12}C, 400 AMeV ^{12}C, 400 AMeV ^{20}Ne and 500 AMeV ^{56}Fe induced different type of emulsion target interactions are studied, we want to find out the general characteristics of the multiplicity distributions and correlations of target fragments at intermediate and high energies.

2 Experimental details

Five stacks of nuclear emulsion made by Institute of Modern Physics, Shanxi Normal University, China, are used in present investigation. The emulsion stacks were exposed horizontally at HIMAC NIRS, Japan. The beams were 150 AMeV ^{4}He, 290 AMeV ^{12}C, 400 AMeV ^{12}C, 400 AMeV ^{20}Ne and 500 AMeV ^{56}Fe respectively, and the flux was 3000 ions/cm^{2}. BA2000 and XSJ-2 microscopes with a 100× oil immersion objective and 10× ocular lenses were used to scan the plates. The tracks were picked up at a distance of 5 mm from the edge of the plates and were carefully followed until they either interacted with emulsion nuclei or escaped from the plates. Interactions which were within 30 μm from the top or bottom surface of the emulsion plates were not considered for final analysis. All the primary tracks were followed back to ensure that the events chosen do not include interactions from the secondary tracks of other interactions. When they were observed to do so the corresponding events were removed from the sample.

In each interaction all of the secondaries were recorded, which include shower particles, target recoiled protons, target evaporated fragments and projectile fragments. According to the emulsion terminology[34], the particles emitted from high energy nucleus-emulsion interactions are classified as follows.

(a) Black track particle ($N_{\rm b}$). They are target evaporated fragments with ionization $I>9I_0$, I_0 being the minimum ionization of a single charged particles. Range of black particle in nuclear emulsion is $R<3$ mm, velocity is $v<0.3c$, and energy is $E<26$ MeV. The multiplicity of black track particle is denoted as $n_{\rm b}$.

(b) Grey track particle ($N_{\rm g}$). They are mostly recoil protons in the kinetic energy range $26\leqslant E\leqslant$ 375 MeV and a few kaons of kinetic energies $20\leqslant E\leqslant$ 198 MeV and pions with kinetic energies $12\leqslant E\leqslant 56$ MeV. They have ionization $1.4I_0\leqslant I\leq 9I_0$. Their ranges in emulsion are greater than 3 mm and have velocities within $0.3c\leqslant v\leqslant 0.7c$. The multiplicity of grey track particle is denoted as $n_{\rm g}$.

The grey and black track particles together are called heavy ionizing particles ($N_{\rm h}$). The multiplicity of heavy ionizing particle is denoted as $n_{\rm h}$.

(c) Shower particle ($N_{\rm s}$). They are produced single-charged relativistic particles having velocity $v\geqslant 0.7c$. Most of them belong to pions contaminated with small proportions of fast protons and K mesons. It should be mentioned that for nucleus-emulsion interactions at a few hundred MeV/nucleon most of shower particles are projectile protons not pions.

(d) The projectile fragments ($N_{\rm f}$) are a different class of tracks with constant ionization, long range, and small emission angle.

The nuclear emulsion is composed of a homogeneous mixture of nuclei. The chemical composition of nuclear emulsion is H, C, N, O, S, I, Br, and Ag, and major composition is H, C, N, O, Br, and Ag. According to the value of $n_{\rm h}$ the interactions are divided into following three groups.

Events with $n_{\rm h}\leqslant 1$ are due to interactions with H target and peripheral interactions with CNO and AgBr targets.

Events with $2\leqslant n_{\rm h}\leqslant 7$ are due to interactions with CNO targets and peripheral interactions with AgBr targets.

Events with $n_{\rm h}\geqslant 8$ definitely belong to interactions with AgBr targets.

3 Results and discussion

Fig. 1 and Fig. 2 show the multiplicity distributions of black and grey track particles in different type of 150 AMeV ^{4}He, 290 AMeV ^{12}C, 400 AMeV ^{12}C, 400 AMeV ^{20}Ne and 500 AMeV ^{56}Fe induced nuclear emulsion interactions, respectively. It is found that with increase of target size the distribution is widened and the position of maximum is increased for the same projectile, no obvious projectile size and energy dependence is observed in

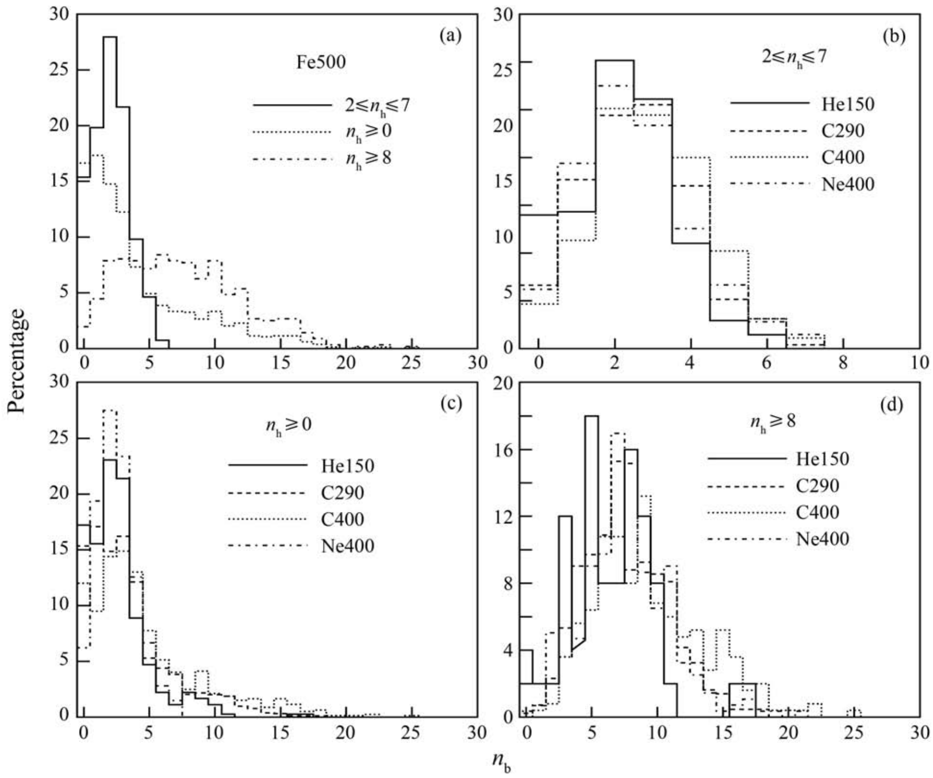

Fig. 1　Multiplicity distribution of black track particle produced in different types of heavy ion induced emulsion target interactions.

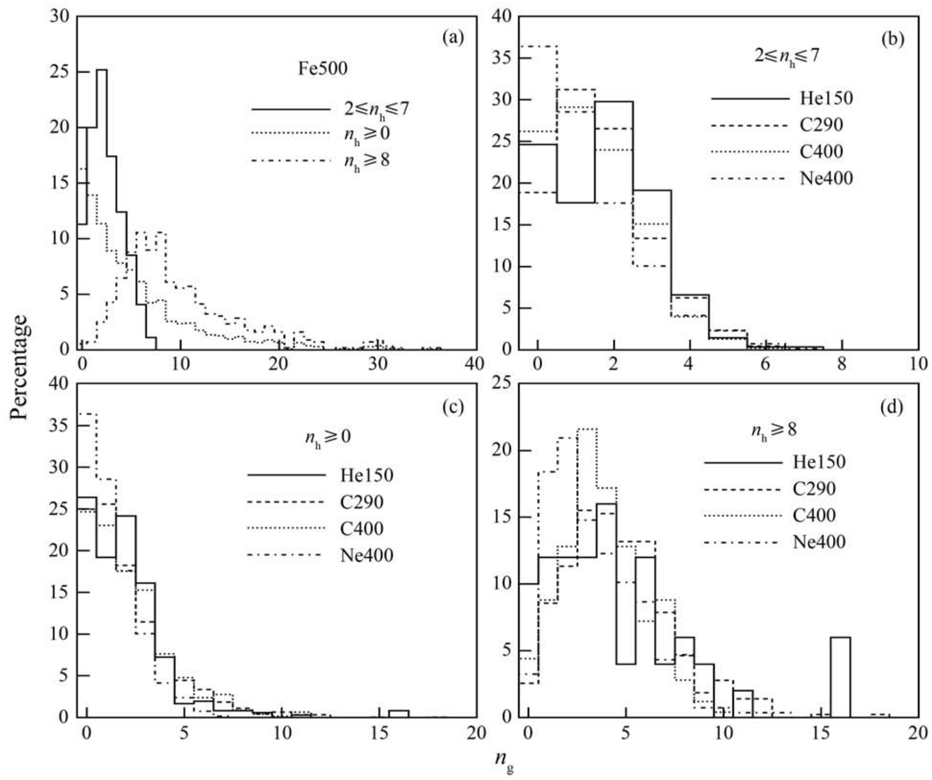

Fig. 2　Multiplicity distribution of grey track particle produced in different types of heavy ion induced emulsion target interactions.

distribution of black track particle for the same target. For light projectile (^{4}He, ^{12}C, and ^{20}Ne) the grey track particle multiplicity distribution does not depend on the type of interactions, but for interaction of heavy projectile and heavy target, such as ^{56}Fe-AgBr, the distribution is broadened. Fig. 3 shows the multiplicity distribution of heavily ionized track particle produced in 150 *A*MeV ^{4}He, 290 *A*MeV ^{12}C, 400 *A*MeV ^{12}C, 400 *A*MeV ^{20}Ne and 500 *A*MeV ^{56}Fe induced nuclear emulsion interactions, comparing to the light projectile (^{4}He, ^{12}C, and ^{20}Ne) the distribution of heavy projectile (^{56}Fe) have a long tail. The averaged multiplicity of black, grey, and heavily ionized track particles in different type of 150 *A*MeV ^{4}He, 290 *A*MeV ^{12}C, 400 *A*MeV ^{12}C, 400 *A*MeV ^{20}Ne and 500 *A*MeV ^{56}Fe induced nuclear emulsion interactions are presented in Table 1. For comparison the corresponding results[28] of 390 *A*MeV ^{20}Ne, 480 *A*MeV ^{40}Ar, and 580 *A*MeV ^{56}Fe induced different type of emulsion target interactions are also listed. It is found that for the same target interactions the averaged black track particle multiplicity is the same within experimental errors for different projectile and energy. For light projectile and light target interaction the averaged grey track particle multiplicity is consistent within experimental errors, but for interaction of ^{56}Fe-AgBr the averaged grey track multiplicity is greater than that of light projectile induced AgBr interactions.

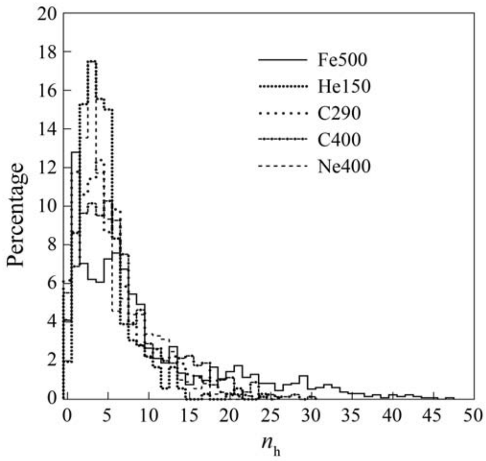

Fig. 3 Multiplicity distribution of heavily ionized track particle produced in different types of heavy ion induced emulsion target interactions.

Table 1 Averaged multiplicity of black, grey and heavily ionized track particles for heavy ion induced different type of emulsion target interactions.

Type of interaction	N_{ev}	$<n_b>$	$<n_g>$	$<n_h>$	Reference
150 *A*MeV ^{4}He-H	38	0.42±0.08	0.39±0.08	0.82±0.06	Present work
150 *A*MeV ^{4}He-CNO	272	2.21±0.08	1.73±0.08	3.94±0.09	Present work
150 *A*MeV ^{4}He-AgBr	50	6.56±0.48	4.58±0.56	11.14±0.53	Present work
150 *A*MeV ^{4}He-Em	360	2.62±0.13	1.99±0.12	4.61±0.18	Present work
290 *A*MeV ^{12}C-H	332	0.36±0.03	0.29±0.02	0.66±0.03	Present work
290 *A*MeV ^{12}C-CNO	1086	2.59±0.04	1.64±0.04	4.23±0.05	Present work
290 *A*MeV ^{12}C-AgBr	432	7.66±0.16	4.60±0.13	12.26±0.18	Present work
290 *A*MeV ^{12}C-Em	1850	3.37±0.07	2.09±0.05	5.46±0.11	Present work
400 *A*MeV ^{12}C-H	99	0.24±0.04	0.31±0.05	0.56±0.05	Present work
400 *A*MeV ^{12}C-CNO	450	2.92±0.07	1.46±0.06	4.39±0.08	Present work
400 *A*MeV ^{12}C-AgBr	250	9.39±0.27	3.96±0.15	13.35±0.30	Present work
400 *A*MeV ^{12}C-Em	799	4.62±0.15	2.10±0.07	6.72±0.19	Present work
400 *A*MeV ^{20}Ne-H	140	0.54±0.04	0.14±0.03	0.68±0.04	Present work
400 *A*MeV ^{20}Ne-CNO	676	2.55±0.06	1.28±0.08	3.83±0.06	Present work
400 *A*MeV ^{20}Ne-AgBr	277	7.75±0.20	3.51±0.14	11.26±0.18	Present work
400 *A*MeV ^{20}Ne-Em	1093	3.61±0.10	1.70±0.06	5.31±0.12	Present work
500 *A*MeV ^{56}Fe-H	223	0.43±0.03	0.32±0.03	0.76±0.03	Present work
500 *A*MeV ^{56}Fe-CNO	540	2.08±0.06	2.47±0.07	4.55±0.07	Present work
500 *A*MeV ^{56}Fe-AgBr	558	7.53±0.19	9.89±0.26	17.42±0.38	Present work
500 *A*MeV ^{56}Fe-Em	1321	4.10±0.12	5.24±0.16	9.35±0.25	Present work
390 *A*MeV ^{20}Ne-H	37	0.14±0.06	0.59±0.08	0.73	[28]
390 *A*MeV ^{20}Ne-CNO	96	2.89±0.12	1.54±0.15	4.43	[28]
390 *A*MeV ^{20}Ne-AgBr	163	5.31±0.42	3.54±0.32	8.85	[28]
390 *A*MeV ^{20}Ne-Em	296	3.88±0.25	2.52±0.19	6.40	[28]
480 *A*MeV ^{40}Ar-H	23	0.61±0.10	0.17±0.08	0.78	[28]

Table 1 (Continued)

Type of interaction	$N_{\rm ev}$	$<n_{\rm b}>$	$<n_{\rm g}>$	$<n_{\rm h}>$	Reference
480 AMeV ^{40}Ar-CNO	63	2.94±0.17	1.16±0.15	4.10	[28]
480 AMeV ^{40}Ar-AgBr	116	5.87±0.48	4.38±0.51	10.25	[28]
480 AMeV ^{40}Ar-Em	202	4.36±0.31	2.90±0.32	7.26	[28]
580 AMeV ^{56}Fe-H	71	0.36±0.07	0.62±0.16	0.98	[28]
580 AMeV ^{56}Fe-CNO	218	2.43±0.14	2.26±0.17	4.69	[28]
580 AMeV ^{56}Fe-AgBr	322	7.98±0.38	8.17±0.69	16.15	[28]
580 AMeV ^{56}Fe-Em	611	5.11±0.27	5.18±0.31	10.29	[28]

The multiplicity correlations between slow particles emitted in heavy ion induced different type of emulsion target interactions are the most sensitive sources of the information about the mechanism of target fragments production. Figs. 4 ∼ 6 show the multiplicity correlations between the different type of target fragments produced in 150 AMeV ^{4}He, 290 AMeV ^{12}C, 400 AMeV ^{12}C, 400 AMeV ^{20}Ne and 500 AMeV ^{56}Fe induced different types of emulsion target interactions. The experimental results can be well represented by a linear relation of the formula

$$\langle n_i\rangle = a n_j + b \ , \tag{1}$$

where $i \neq j$ means black track particle (b), grey track particle (g) and heavily ionized track particle (h), respectively. The correlation parameters a and b obtained by the least-square fitting are listed in Table 2. It should be mentioned that some of the fitting parameters are from the first a few data sets. It can be seen that for heavy ion induced light targets (CNO) interactions $\langle n_{\rm b}\rangle$ decreases with the increase of $n_{\rm g}$ and $\langle n_{\rm g}\rangle$ decreases with the increase of $n_{\rm b}$. For heavy ion induced heavy targets (AgBr) interactions $\langle n_{\rm g}\rangle$ decreases firstly and then keeps constant with increase of the value of $n_{\rm b}$ except for the case of 500 AMeV ^{56}Fe where $\langle n_{\rm g}\rangle$ decreases firstly then increases and finally becomes saturation with the increase of n_b, $\langle n_{\rm b}\rangle$ also decreases firstly and then becomes constant with increase of the value of $n_{\rm g}$ except for the case of 500 AMeV ^{56}Fe where $\langle n_{\rm b}\rangle$ decreases firstly then increases and finally becomes constant with the increase of $n_{\rm g}$. For other type of interactions the positive multiplicity correlations are observed except for correlation between $\langle n_{\rm b}\rangle$ and $n_{\rm g}$ for 500 AMeV ^{56}Fe induced emulsion interactions where $\langle n_{\rm b}\rangle$ increases firstly and then becomes saturation with increase of $n_{\rm g}$, and for correlation between $\langle n_{\rm b}\rangle$ and $n_{\rm g}$, and correlation of $\langle n_{\rm g}\rangle$ with $n_{\rm b}$ for

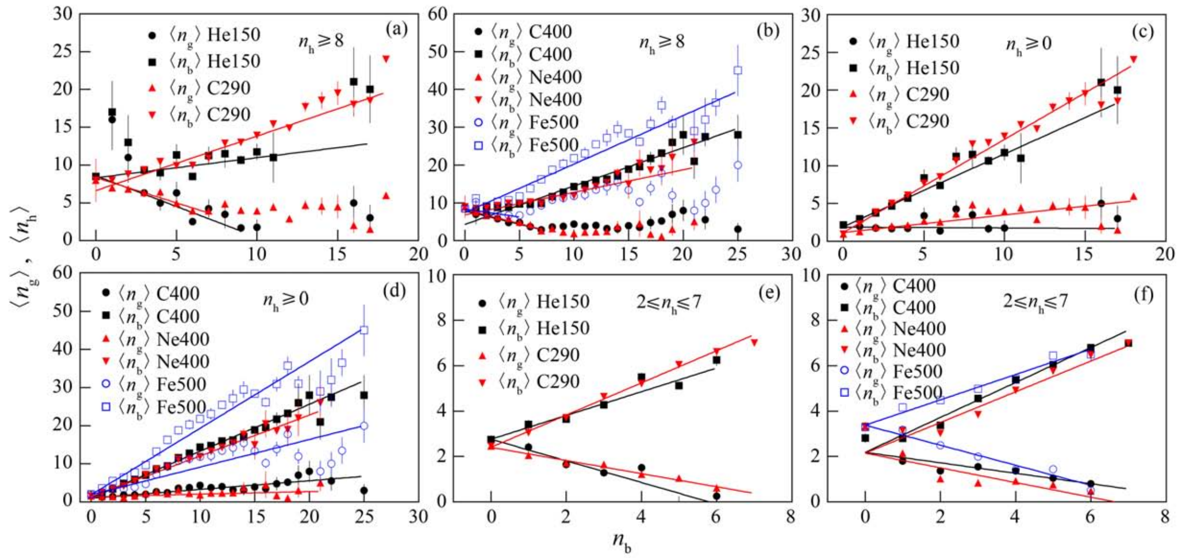

Fig. 4 (color online) Dependences of the averaged multiplicity of grey and heavily ionized track particles on the number of black track particle.

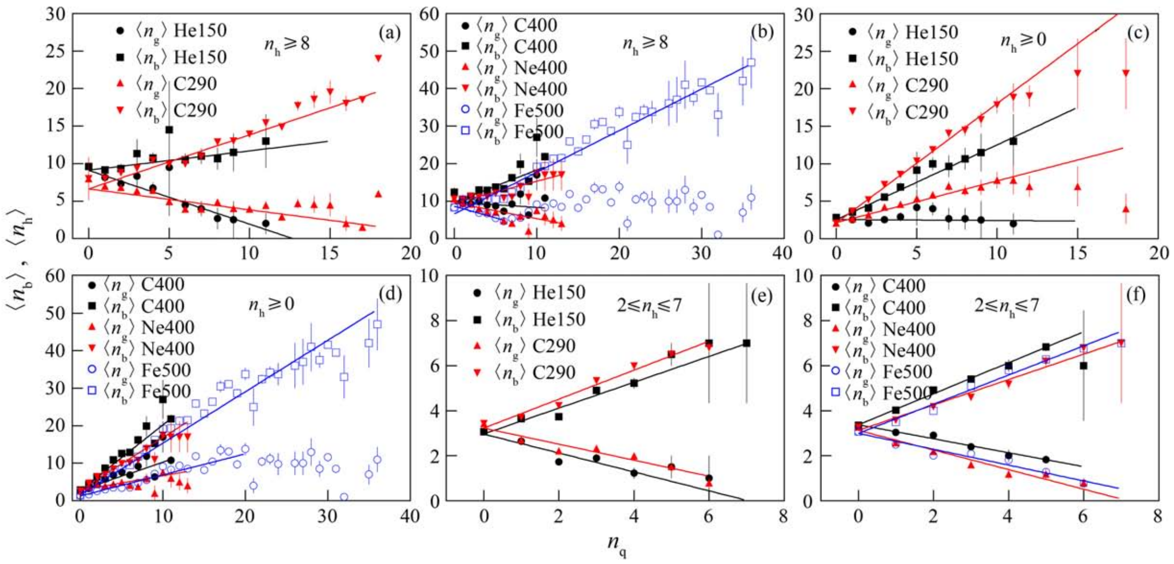

Fig. 5　(color online) Dependences of the averaged multiplicity of black and heavily ionized track particles on the number of grey track particle.

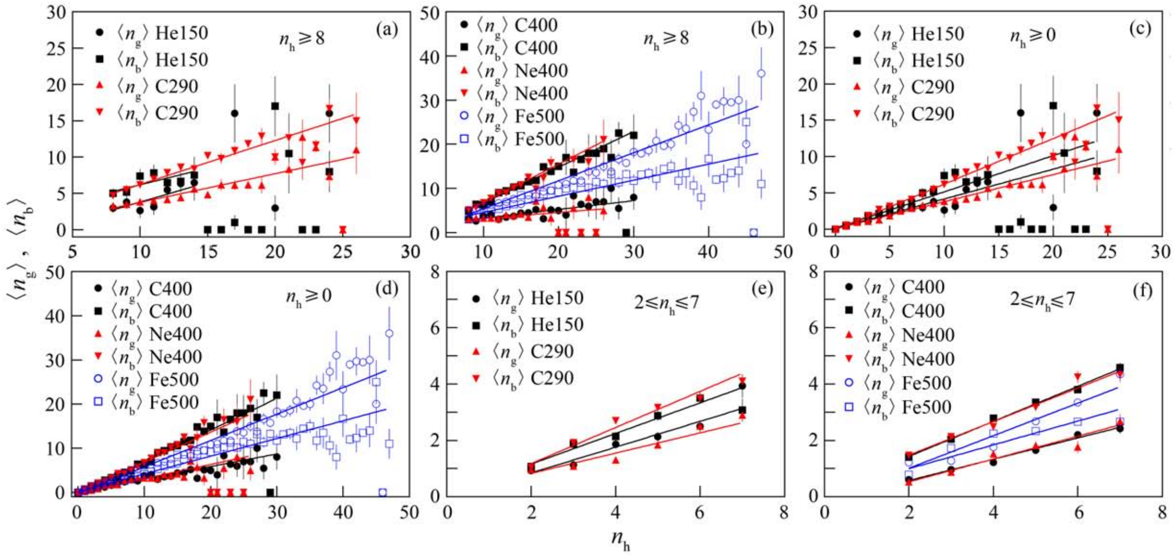

Fig. 6　(color online) Dependences of the averaged multiplicity of black and grey track particles on the number of heavily ionized track particle.

Table 2　Parameters of multiplicity correlation for heavy ion induced different type of emulsion targets interactions.

Beam	Type of correlation	$2\leqslant n_h\leqslant 7$		$n_h\geqslant 8$		$n_h\geqslant 0$	
		a	b	a	b	a	b
150 AMeV ^{4}He	$\langle n_b\rangle - n_g$	−0.420±0.052	2.959±0.115	−0.716±0.082	9.085±0.280	−0.012±0.069	2.559±0.166
290 AMeV ^{12}C	$\langle n_b\rangle - n_g$	−0.356±0.020	3.226±0.059	−0.356±0.049	9.334±0.238	0.556±0.032	2.160±0.078
400 AMeV ^{12}C	$\langle n_b\rangle - n_g$	−0.310±0.037	3.374±0.095	−0.140±0.078	9.722±0.362	0.743±0.057	2.826±0.156
400 AMeV ^{20}Ne	$\langle n_b\rangle - n_g$	−0.436±0.028	3.127±0.070	−0.421±0.052	9.533±0.254	0.387±0.036	2.815±0.095
500 AMeV ^{56}Fe	$\langle n_b\rangle - n_g$	−0.352±0.021	2.992±0.087	−0.617±0.078	8.610±0.295	0.560±0.018	1.305±0.077
150 AMeV ^{4}He	$\langle n_h\rangle - n_g$	0.574±0.052	2.966±0.115	0.257±0.094	9.124±0.287	0.998±0.076	2.545±0.172
290 AMeV ^{12}C	$\langle n_h\rangle - n_g$	0.644±0.020	3.226±0.059	0.627±0.052	9.389±0.238	1.592±0.033	2.116±0.079
400 AMeV ^{12}C	$\langle n_h\rangle - n_g$	0.689±0.037	3.357±0.095	0.853±0.078	9.740±0.362	1.739±0.057	2.830±0.156
400 AMeV ^{20}Ne	$\langle n_h\rangle - n_g$	0.564±0.028	3.127±0.070	0.575±0.055	9.543±0.257	1.405±0.037	2.799±0.096

Table 2 (Continued)

Beam	Type of correlation	$2\leqslant n_h\leqslant 7$		$n_h\geqslant 8$		$n_h\geqslant 0$	
		a	b	a	b	a	b
500 AMeV ^{56}Fe	$\langle n_h\rangle-n_g$	0.648±0.021	2.992±0.087	1.100±0.015	6.595±0.186	1.370±0.011	1.658±0.073
150 AMeV ^{4}He	$\langle n_g\rangle-n_b$	−0.477±0.034	2.760±0.122	−0.811±0.075	8.577±0.395	−0.011±0.042	1.894±0.146
290 AMeV ^{12}C	$\langle n_g\rangle-n_b$	−0.290±0.016	2.401±0.060	−0.752±0.113	8.640±0.519	0.232±0.014	1.178±0.050
400 AMeV ^{12}C	$\langle n_g\rangle-n_b$	−0.230±0.027	2.180±0.108	−0.708±0.084	7.878±0.438	0.228±0.011	1.023±0.072
400 AMeV ^{20}Ne	$\langle n_g\rangle-n_b$	−0.324±0.024	2.146±0.086	−0.761±0.061	8.276±0.260	0.070±0.013	1.357±0.075
500 AMeV ^{56}Fe	$\langle n_g\rangle-n_b$	−0.441±0.036	3.378±0.118	−0.419±0.090	8.357±0.193	0.850±0.040	1.707±0.116
150 AMeV ^{4}He	$\langle n_h\rangle-n_b$	0.523±0.034	2.760±0.122	0.265±0.067	8.319±0.381	0.961±0.045	1.954±0.151
290 AMeV ^{12}C	$\langle n_h\rangle-n_b$	0.710±0.016	2.401±0.061	0.721±0.029	6.621±0.243	1.232±0.014	1.178±0.050
400 AMeV ^{12}C	$\langle n_h\rangle-n_b$	0.770±0.027	2.180±0.108	1.014±0.017	4.375±0.195	1.230±0.011	1.108±0.073
400 AMeV ^{20}Ne	$\langle n_h\rangle-n_b$	0.676±0.024	2.146±0.086	0.597±0.020	6.820±0.176	1.073±0.014	1.350±0.076
500 AMeV ^{56}Fe	$\langle n_h\rangle-n_b$	0.559±0.036	3.378±0.118	1.284±0.032	7.420±0.156	1.747±0.029	1.868±0.108
150 AMeV ^{4}He	$\langle n_g\rangle-n_h$	0.457±0.046	−0.073±0.178	0.541±0.212	−1.598±2.115	0.409±0.026	0.081±0.090
290 AMeV ^{12}C	$\langle n_g\rangle-n_h$	0.359±0.020	0.110±0.075	0.394±0.027	−0.174±0.331	0.373±0.008	0.065±0.029
400 AMeV ^{12}C	$\langle n_g\rangle-n_h$	0.378±0.028	−0.183±0.115	0.198±0.029	1.276±0.379	0.284±0.011	0.208±0.054
400 AMeV ^{20}Ne	$\langle n_g\rangle-n_h$	0.405±0.030	−0.285±0.094	0.135±0.047	1.846±0.531	0.321±0.012	−0.084±0.038
500 AMeV ^{56}Fe	$\langle n_g\rangle-n_h$	0.578±0.028	−0.148±0.116	0.633±0.011	−0.925±0.192	0.598±0.006	−0.208±0.035
150 AMeV ^{4}He	$\langle n_b\rangle-n_h$	0.543±0.046	0.073±0.178	0.459±0.212	1.598±2.117	0.499±0.025	0.154±0.088
290 AMeV ^{12}C	$\langle n_b\rangle-n_h$	0.641±0.020	−0.110±0.075	0.606±0.027	0.173±0.331	0.627±0.008	−0.065±0.029
400 AMeV ^{12}C	$\langle n_b\rangle-n_h$	0.622±0.028	0.181±0.115	0.806±0.030	−1.315±0.388	0.716±0.011	−0.207±0.055
400 AMeV ^{20}Ne	$\langle n_b\rangle-n_h$	0.595±0.030	0.285±0.094	0.868±0.050	−1.885±0.556	0.677±0.012	0.087±0.038
500 AMeV ^{56}Fe	$\langle n_b\rangle-n_h$	0.422±0.028	0.148±0.116	0.364±0.010	0.973±0.191	0.400±0.006	0.214±0.035

150 AMeV ^{4}He induced emulsion interactions where the slope parameters are -0.012 ± 0.069, and -0.011 ± 0.042 respectively, the fitted error is big because of the limited statistics.

Based on the participant-spectator model[32−33] and the cascade evaporation model[34] of high energy nucleus-nucleus collisions, the grey track particles are emitted from the target nucleus very soon after the instant of impact, which is the target recoiled protons of energy ranging up to 400 MeV, the black track particles are images of target evaporated particles of low-energy($E<30$ MeV) and singly or multiply charged fragments. On the average, with the increase of the number of cascading collisions the excitation energy of target residues increases, so $\langle n_b\rangle$ (or $\langle n_g\rangle$) increases with the increase of n_g (or n_b).

For interactions with $2\leqslant n_h\leqslant 7$, $\langle n_g\rangle$ decreases with increase of n_b, and $\langle n_b\rangle$ decreases with increase of n_g owing to the limited target size (the maximum target fragments $n_h=8$ which corresponds to total disintegration of oxygen nucleus).

For light projectile (such as ^{4}He, ^{12}C, and ^{20}Ne) induced heavy target(AgBr) interactions, with increasing of n_b the excitation energy of target residues and the number of cascading collisions are increased, but owing to the limited projectile the number of cascading collisions and the excitation energy of target residues are limited, and owing to the limitation of nuclear emulsion detector the peripheral or semi-central AgBr target interactions ($n_h\leqslant 7$) can not be discriminated with H and CNO targets interactions, this type of the interaction is classified into the interactions with H target and CNO target interactions, so $\langle n_g\rangle$ decreases firstly and then keeps constant with increase of n_b and $\langle n_b\rangle$ also decreases firstly and then becomes constant with increase of n_g.

It should be mentioned that the correlation between $\langle n_b\rangle$ (or $\langle n_g\rangle$) and n_g (or n_b) for 500 AMeV ^{56}Fe-AgBr interactions is different from that for light projectile induced AgBr interactions. Generally speaking, it is true that with the increase of the number of cascading collisions the excitation energy of target residues increases, so $\langle n_\mathrm{b}\rangle$ (or $\langle n_\mathrm{g}\rangle$) increases with the increase of n_g (or n_b). Because of the limitation of nuclear emulsion detector, the peripheral or semi-central Fe-AgBr target interactions with $n_\mathrm{h} \leqslant 7$ is not included in the type of Fe-AgBr target interactions and which is classified into Fe-H and Fe-CNO target interactions, so $\langle n_\mathrm{b}\rangle$ (or $\langle n_\mathrm{g}\rangle$) decreases firstly with the increase of n_g (or n_b). When the effect of the limitation of nuclear emulsion detector is finished, the real interaction characteristics is appeared that $\langle n_\mathrm{b}\rangle$ (or $\langle n_\mathrm{g}\rangle$) increases with the increase of n_g (or n_b). Finally because of the limitation of target residue size, the number of cascading collisions and the excitation energy of target residues are limited, so $\langle n_\mathrm{b}\rangle$ (or $\langle n_\mathrm{g}\rangle$) becomes constant with the increase of n_g (or n_b).

For interactions with $n_\mathrm{h} \geqslant 0$ (all of the targets), $\langle n_\mathrm{g}\rangle$ increases with increase of n_b, and $\langle n_\mathrm{b}\rangle$ increases with increase of n_g, because with the increase of the number of cascading collisions the excitation of target residues increases. For the correlations of $\langle n_h\rangle$ and n_g, $\langle n_\mathrm{h}\rangle$ and n_b, $\langle n_\mathrm{b}\rangle$ and n_h, $\langle n_\mathrm{g}\rangle$ and n_h for all type of interactions, positive linear correlation is of course existed, because n_h is the sum of n_b and n_g, with increase of n_b or n_g the $\langle n_\mathrm{h}\rangle$ is increased, and with increase of n_h the values of $\langle n_\mathrm{g}\rangle$ and $\langle n_\mathrm{b}\rangle$ are also increased. All of these multiplicity correlation effects for interactions with $n_\mathrm{h} \geqslant 0$ are the same as that observed in high energy nucleus-emulsion interactions.

4 Conclusions

The multiplicity distributions and correlations of black, grey and heavily ionized track particles emitted in 150 AMeV ^{4}He, 290 AMeV ^{12}C, 400 AMeV ^{12}C, 400 AMeV ^{20}Ne and 500 AMeV ^{56}Fe induced different type of nuclear emulsion interactions are investigated. It is found that the averaged multiplicity of grey, black and heavily ionized track particle increase with the increase of target size. For the same target the averaged black track particle multiplicity does not depend on the projectile size and energy, and the averaged grey track particle multiplicity also does not depend on the the projectile size and energy for light projectile, but for heavy projectile such as ^{56}Fe the averaged grey track particle multiplicity is increased evidently. There is a linear correlation between the multiplicity of different target fragments. The experimental results can be well explained based on the geometrical picture and the cascade evaporation model of nucleus-nucleus interactions.

References:

[1] BUBNOV V I, GAITINOV A S, EREMENKO L E, *et al.* (Alma-Ata-Bucharest-Dubna-Dushanbe-Kishinev-Kosice-Leningrad-Moscow-Tashkent-Ulaan-Bator Collaboration). Z Phys A, 1981, **302**: 133.

[2] STENLUND E, OTTERLUND I. Nucl Phys B, 1982, **198**: 407.

[3] FERRARI A, RANFT J, ROESLER S, SALA P R. Z Phys C, 1996, **70**: 413.

[4] ADAMOVICH M I, AGGARWAL M M, ALEXANDROV Y A, *et al.* (EMU01 Collaboration). Z Phys C, 1995, **65**: 421.

[5] ABD ALLAH N N. Phys Scri, 1996, **54**: 436.

[6] EL-NAGHY A, ABOU-STEIT S A H, ABDEL-AZIZ S S, *et al.* Heavy Ion Phys, 2002, **15**: 131.

[7] KHAN M S, KHUSHOOD H, ANSARI A R. Can J Phys, 1996, **74**: 651.

[8] AHMAD M S, KHAN M Q R, SIDDIQUE K A, *et al.* Intern J Mod Phys A, 1995, **10**: 845.

[9] ABDAL-HALIM S M, ABDEL-WAGED K. Nucl Phys A, 2004, **730**: 419.

[10] KHAN M Q R, AHMAD M S, SIDDIQUE K A, *et al.* Nuovo Cim A, 1988, **99**: 417.

[11] AHMAD T, IRFAN M. Nuovo Cim A, 1993, **106**: 171.

[12] GHOSH D, MUKHOPADHYAY A, GHOSH A, *et al.* Nucl Phys A, 1989, **499**: 850.

[13] GHOSH D, ROY J, SENGUPTA R. Nucl Phys A, 1987, **468**: 719.

[14] MOHERY M, ABD-ALLAH N N. Intern J Mod Phys E, 2002, **11**: 161.

[15] ADAMOVICH M I, AGGARWAL M M, ALEXANDROV Y A, *et al.* (EMU01 Collaboration). Z Phys A, 1997, **358**: 337.

[16] ABD-ALLAH N N, LIU Fuhu, SULTAN E A, *et al.* Pramana J Phys, 2013, **8**: 281.

[17] GILL A, BHALLA K B, KUMAR V, *et al.* Intern J Mod Phys A, 1990, **5**: 755.

[18] NASR M A, KHUSHOOD H. Intern J Mod Phys A, 1994, **9**: 5145.

[19] AHMAD S, AHMAD M A, TARIQ M, *et al.* Intern J Mod Phys E, 2009, **18**: 1929.

[20] TARIQ M, ZAFAR M, TUFAIL A, *et al.* Intern J Mod Phys E, 1995, **4**: 347.

[21] JILARY M A, ABD-ALLAH N N, ABD-ELDAIM A. Intern J Mod Phys E, 1995, **4**: 815.

[22] EL-NADI M, METTWALLI N, SHAAT E A, *et al.* Intern J Mod Phys E, 1996, **5**: 617.

[23] EL-NADI M, EL-NAGHY M S, SHAAT E A, *et al.* Intern J Mod Phys E, 1997, **6**: 135.

[24] EL-NADI M, ABDEL S A, HUSSEIN A, *et al.* Intern J Mod Phys E, 1997, **6**: 191.

[25] LI Huiling, ZHANG Donghai, LI Xueqin, *et al.* Atomic Energy Sci Tech, 2008, **42**: 488.(in Chinese)
(李惠玲, 张东海, 李雪琴, 等. 原子能科学技术，2008，**42**: 488.)

[26] ZHANG Donghai, LUO Shibin. High Energy Phys Nucl Phys, 1992, **16**: 340.(in Chinese)
(张东海, 罗世彬. 高能物理与核物理, 1992, **16**: 340.)

[27] ZHANG Donghai. High Energy Phys and Nucl Phys, 2001, **25**: 651.(in Chinese)
(张东海. 高能物理与核物理, 2001, **25**: 651.)

[28] DUDKIN V E, KOVALEV E E, NEFEDOV N A, *et al.* Nucl Phys A, 1994, **568**: 906.

[29] LI Junsheng, ZHANG Donghai, LI Huiling. Atomic Energy Sci Tech, 2013, **47**: 907.(in Chinese)
(李俊生, 张东海, 李惠玲. 原子能科学技术, 2013, **47**: 907.)

[30] JAKOBSSON B, JONSSON G, KARLSSON L, *et al.* Nucl Phys A, 1990, **509**: 195.

[31] ZHANG D H, CHEN Y L, WANG G R, *et al.* [EB/OL]. [2014-04-01]. http://arXiv.org/abs/1403.3897.

[32] HUFNER J, SCHAFER K, SCHURMANN B. Phys Rev C, 1975, **12**: 1888.

[33] BOWMAN J D, SWIATECKI W J, TSANG C F. Abrasion and ablation of heavy ions [R], Lawrence Berkeley Report: LBL-2098, 1973.

[34] POWELL P L, FOWLER P H. The study of elementary particles by photographic method[M]. Oxford: Pergamon, 1959.

中高能重离子诱发乳胶核反应慢粒子产生

张东海[1)]，陈艳玲，王国蓉，李王东，王 青，姚继杰，周建国，李 蓉，李俊生，李惠玲

(山西师范大学现代物理研究所，山西 临汾 041004)

摘要: 对150 *A*MeV ^{4}He，290 *A*MeV ^{12}C，400 *A*MeV ^{12}C，400 *A*MeV ^{20}Ne及500 *A*MeV ^{56}Fe诱发乳胶不同靶核反应靶核碎片多重数分布及关联进行了研究。结果表明，黑径迹粒子、灰径迹粒子及重电离粒子平均多重数随靶核大小的增加而增加，不同靶核碎片多重数之间存在线性关联。这些实验结果均可以依据核-核碰撞几何模型及级联蒸发模型来解释。

关键词: 重离子碰撞; 靶核碎片; 多重数; 关联; 原子核乳胶

收稿日期: 2014-04-20; **修改日期:** 2014-04-28

基金项目: 国家自然科学基金资助项目(11075100)；山西省自然科学基金资助项目(2011011001-2)；山西省留学归国人员基金资助项目(2011-058)

1) E-mail: zhangdh@dns.sxnu.edu.cn。